THE JOURNAL OF BIOLOGICAL CHEMISTRY
Vol. 273, No. 25, Issue of June 19, pp. 15404–15411, 1998
Printed in U.S.A.

The Two [4Fe-4S] Clusters in *Chromatium vinosum* Ferredoxin Have Largely Different Reduction Potentials

STRUCTURAL ORIGIN AND FUNCTIONAL CONSEQUENCES*

(Received for publication, December 5, 1997, and in revised form, April 1, 1998)

Panayotis Kyritsis‡, Oliver M. Hatzfeld§, Thomas A. Link§, and Jean-Marc Moulis‡¶

From the ‡CEA, Département de Biologie Moléculaire et Structurale, Laboratoire Métalloprotéines, 17 rue des Martyrs, 38054 Grenoble Cedex 9, France and §Institut für Biochemie I, Molekulare Bioenergetik, Universitätklinikum Frankfurt, ZBC, D-60590 Frankfurt/Main, Germany

The 2[4Fe-4S] ferredoxin from *Chromatium vinosum* arises as one prominent member of a recently defined family of proteins found in very diverse bacteria. The potentiometric circular dichroism titrations of the protein and of several molecular variants generated by site-directed mutagenesis have established that the reduction potentials of the two clusters differ widely by almost 200 mV. This large difference has been confirmed by electrochemical methods, and each redox transition has been assigned to one of the clusters. The unusually low potential center is surprisingly the one that displays a conventional CX^1X^2CX^3X^4C (X^n, variable amino acid) binding motif and a structural environment similar to that of clusters having less negative potentials. A comparison with other ferredoxins has highlighted factors contributing to the reduction potential of [4Fe-4S] clusters in proteins. (i) The loop between the coordinating cysteines 40 and 49 and the C terminus α-helix of *C. vinosum* ferredoxin cause a negative, but relatively moderate, shift of ~60 mV for the nearby cluster. (ii) Very negative potentials, below −600 mV, correlate with the presence of a bulky side chain in position X^4 of the coordinating triad of cysteines. These findings set the framework in which previous observations on ferredoxins can be better understood. They also shed light onto the possible occurrence and properties of very low potential [4Fe-4S] clusters in less well characterized proteins.

[4Fe-4S] clusters are present in a wide variety of proteins; they are often coordinated to amino acids organized in characteristic motifs (1) corresponding to protein domains, sometimes identified by x-ray crystallography (see Ref. 2 and references therein). A pair of [4Fe-4S] clusters is found in many bacterial ferredoxins (3) and other electron transfer proteins and enzymes (see Fig. 1 in Ref. 4). In most cases these clusters are bound to the proteins through a pair of C*XXCXX*C . . . CP (*X*, variable amino acid) motifs containing all necessary cysteine ligands. Extensive work on the simplest ferredoxins over the last 35 years has established that the two clusters are relatively close, at a distance of approximately 10 Å thus enabling them to interact magnetically, and that they display similar reduction potentials, generally around −400 ± 100 mV (normal hydrogen electrode). Until now, these generic properties have not been conclusively challenged in any fully characterized molecule containing such 2[4Fe-4S] domains. Proteins with homologous coordinating motifs are known in which one of the [4Fe-4S] clusters is substituted by a [3Fe-4S] center, often as a result of the loss of one of the cysteine ligands (5). Consequently, these proteins exhibit properties that are clearly different from those of molecules containing two [4Fe-4S] centers (6).

Recently, the 2[4Fe-4S] ferredoxin from the purple sulfur photosynthetic bacterium *Chromatium vinosum* has been further investigated (7), following its initial characterization (8), in an effort to assess the influence of specific sequence elements (including a 6-amino acid insertion between two cysteine ligands and a long C-terminal extension) on the properties of the [4Fe-4S] clusters. It was found that, in contrast to other 2[4Fe-4S] ferredoxins without these elements, the electronic communication between the two clusters was apparently impaired (7). The gene encoding *C. vinosum* ferredoxin (CvFd)[1] was later cloned and expressed in *Escherichia coli* (9), and the structure of the protein was determined (10). These studies provide the necessary background for exploring the structure-function relationships in CvFd by protein engineering, and this report presents our initial efforts toward this aim.

The properties of Fe-S clusters can be probed by a number of spectroscopic methods. The absorption spectra are generally broad as they result from overlapping charge transfer bands in the visible-near UV range. The resolution of these spectra can be significantly improved by the implementation of circular dichroism (CD) which provides both a characteristic pattern for each cluster type and a sensitive monitor of changes affecting either the cluster or the protein (11). The use of the method as an accurate analytical tool is broadened when the CD spectra of electron transfer proteins can be monitored as a function of the applied potential (12). Indeed, both a measure of the reduction potential and an estimate of the structural changes induced by the addition or removal of electrons are then provided.

The results of such studies, together with direct electrochemical measurements, are reported herein for CvFd and a series of molecular variants. The comparison with the well characterized 2[4Fe-4S] ferredoxin from *Clostridium pasteurianum* (CpFd) reveals that the [4Fe-4S] clusters in CvFd display unusual redox properties which help explain previously observed differences between these proteins (7). These data also provide unprecedented compelling evidence that the protein domains containing two [4Fe-4S] clusters found in widely different biological systems do not always display similar physicochemical and functional properties.

* This work was supported in part by Grant Li 474/7 from the Deutsche Forschungsgemeinschaft. The costs of publication of this article were defrayed in part by the payment of page charges. This article must therefore be hereby marked "*advertisement*" in accordance with 18 U.S.C. Section 1734 solely to indicate this fact.

¶ To whom correspondence should be addressed: CEA/Grenoble, DBMS-MEP, 17 rue des Martyrs, 38054 Grenoble Cedex 9, France. Tel.: 33 476885623; Fax: 33 476885872; E-mail jean-marc.moulis@cea.fr.

[1] The abbreviations used are: CvFd, *Chromatium vinosum* ferredoxin; Cp, *Clostridium pasteurianum*.

TABLE I
Oligonucleotides used to prepare CvFd variants

Molecular variant of CvFd	Sequence (complementary to coding strand)
Y44C/S	5′cgtactgagaggtctcg(C/G)agtgtccgacgc3′
Δ1	5′cttcgacgcactgag-------cgcactcggtgcag3′
K74−/E	5′gctcgtact(A/C)ggcgcgcagctcg3′
Δ1K74−	Assembly of the *Nde*I-*Bam*HI fragment from Δ1 and the *Bam*HI-*Pst*I fragment from K74−
D12G	5′gcatcaattgtgGtgtctgcgagcccg3′[a]
V13G	5′gcatcaattgtgatgGctgcgagcccg3′[a]
Y30F	5′gggttcgatcacaAaggtctcgtcaccc3′

[a] Complementary to non-coding strand. Substituted bases are in capital letters.

EXPERIMENTAL PROCEDURES

Preparation of Proteins—Site-directed mutagenesis was carried out on plasmid pCVFD11 encoding CvFd (9) using two rounds of polymerase chain reaction as described previously (13). The oligonucleotides bearing the mutations are listed in Table I. The plasmids were sequenced with the dideoxynucleotide termination method (14). The genes bearing the correct mutations were expressed in *E. coli* K38/pGP1-2 (15), as described previously (4), and the synthesis of ferredoxin was checked by [^{35}S]cysteine labeling (16). For large scale (20 liters) production, cells were grown at 30 °C until they reached an optical density measured at 600 nm of about 1.5. They were then induced for 1 h at 42 °C, and the synthesis of ferredoxin proceeded for about 5 h at 30 °C before harvest. Purification of the CvFd derivatives was as previously outlined for other 2[4Fe-4S] ferredoxins (17). It is of note that none of the CvFd derivatives studied herein had a significantly different chromatographic behavior compared with the native protein. However, the changes introduced into the amino acid sequence were often easily verified by a range of spectroscopic methods (see below).[2] The 2[4Fe-4S] ferredoxin from *E. coli* (9) was overproduced and similarly purified.

Electrochemistry—Cyclic voltammetry and square wave voltammetry were performed using a previously described device (18). The potential was controlled through an Autolab PGSTAT-10 potentiostat (Deutsche Metrohm, Filderstadt, Germany). The working electrode was a gold disc, the counter electrode a platinum wire, and the reference electrode a standard saturated Ag/AgCl electrode (Radiometer, Copenhagen). All potentials in this work are referenced to the normal hydrogen electrode, taking E(Ag/AgCl) = 197.6 mV. The concentrations of the protein samples were 1–2 mM, in 10 mM potassium phosphate buffer, pH 7.5. An attempt to perform electrochemical studies on a pyridine-3-carboxaldehyde thiosemicarbazone-modified gold electrode was not successful. However, a very good response was obtained in the presence of 0.2 mM viologens; considering the range of potentials investigated, a mixture of methyl viologen (E_1^0 −455 mV) and 4′,4″-dimethyl-1′,1″-trimethylene-2′,2″-dipyridinium dibromide (E_1^0 −680 mV) was used. The working electrode was poised at −800 mV before each voltammogram was taken.

The ionic strength of protein solutions was adjusted by addition of appropriate amounts of concentrated NaCl solution. Studies at different pH values were carried out by diluting small aliquots of recombinant CvFd into a previously detailed Good's buffer solution (12).

Circular Dichroism and Absorption Spectroscopy—The setup for optical measurements and redox titrations was as in previous studies (12). The concentrations of the protein samples for CD spectroscopy in the visible range were 1–2 mM, in 10 mM potassium phosphate buffer, pH 7.5, and contained 0.6 mM each of benzyl viologen (E_1^0 −360 mV), methyl viologen (E_1^0 −445 mV), 1′,1″-trimethylene-2′,2″-dipyridinium dibromide (E_1^0 −550 mV), and 4′,4″-dimethyl-1′,1″-trimethylene-2′,2″-dipyridinium dibromide (E_1^0 −680 mV). The last two compounds were synthesized according to Ref. 19. The potential was applied between 15 and 30 min before recording the CD spectra during titration experiments; it was checked that no further spectral changes occurred after this equilibration time over the potential range investigated. The path lengths of the cells were 0.1 mm for work in the visible range and 10 or 20 μm between 180 and 280 nm. Absorption spectra were similarly recorded, but the solutions contained the protein and the four viologens at concentrations of 0.8 mM and 20 μM, respectively.

Dithionite Reduction of CvFd—Ferredoxin solutions (concentrations of 0.1–0.2 mM) in 20 mM potassium phosphate buffer, pH 8.2, were kept under argon inside an anaerobic chamber (Jacomex, Livry-Gargan, France) ensuring an oxygen concentration of less than 1.5 ppm. The proteins were reduced by the addition of a 30-fold molar excess of sodium dithionite (Eastman Kodak), and absorption spectra were regularly recorded with a Hewlett-Packard model 8453 spectrophotometer and a previously described set-up (4).

[2] P. Kyritsis, O. M. Hatzfeld, T. A. Link, and J.-M. Moulis, unpublished data.

RESULTS

Molecular Variants of CvFd

Fig. 1 highlights the targets for site-directed mutagenesis investigated in CvFd. The first set of variants involves modifications of the protein environment around cluster II which is coordinated by Cys-18, Cys-37, Cys-40, and Cys-49. In the variant referred to as Δ1 the loop (residues 41–48) between two of the cysteine ligands of cluster II (10) has been replaced by two residues (Ala-Gln), therefore converting the sequence to a more conventional binding motif (C*XX*CAQC . . . CP) for [4Fe-4S] clusters. In the K74− variant, half (residues 74–82) of the C-terminal α-helix has been removed. In Δ1K74− the two modifications were combined, and in K74E the buried hydrophilic side chain of lysine (10) has been substituted by glutamic acid. In two more variants, Y44C and Y44S, residue Tyr-44 of loop Δ1 has been replaced by a cysteine or a serine.

The second set of variants, namely D12G, V13G, and Y30F, contains single site replacements introduced close to cluster I which is coordinated by Cys-8, Cys-11, Cys-14, and Cys-53.

Circular Dichroism Spectroscopy

Since CvFd apparently deviates from other 2[4Fe-4S] ferredoxins in its ability to convey intramolecular electron transfer between its clusters (7), evidence for unusual spectroscopic properties was sought using CD spectroscopy.

CD Spectra and Electrochemical Titration of CpFd—For reference, the visible CD spectra recorded during the redox titration of native CpFd are shown in Fig. 2. These data qualitatively confirm and extend previous reports (11, 20). The spectra of the fully oxidized protein with $[4Fe\text{-}4S]^{2+}$ clusters contain several moderately intense features all over the spectral range shown. Upon reduction, a significant decrease in the intensity of all these bands occurs; at −600 mV a positive band with a maximum at 360 nm and a shoulder at 380 nm is the main feature of the spectrum (Fig. 2). In contrast, the far UV region (Fig. 3) shows little, if any, change in the relatively weak negative band around 200 nm. These observations are consistent with the lack of extensive secondary structure elements in clostridial ferredoxins (21). Moreover, they suggest that only small global structural changes are induced by adding one electron to each cluster.

The variation of the intensities of these peaks as a function of the applied potential provides a measure of the reduction potential (Fig. 2, *inset*). In agreement with previous studies (22, 23), a single redox wave, with a midpoint potential of −369 ± 4 mV, is observed between −300 and −600 mV. Moreover, the disappearance of all spectral features associated with oxidized clusters indicates that the two clusters of this protein display the same potential, as expected from a number of previous experiments (24).

CD Spectra and Electrochemical Titration of CvFd—The CD spectra of oxidized CvFd are almost identical to those of CpFd

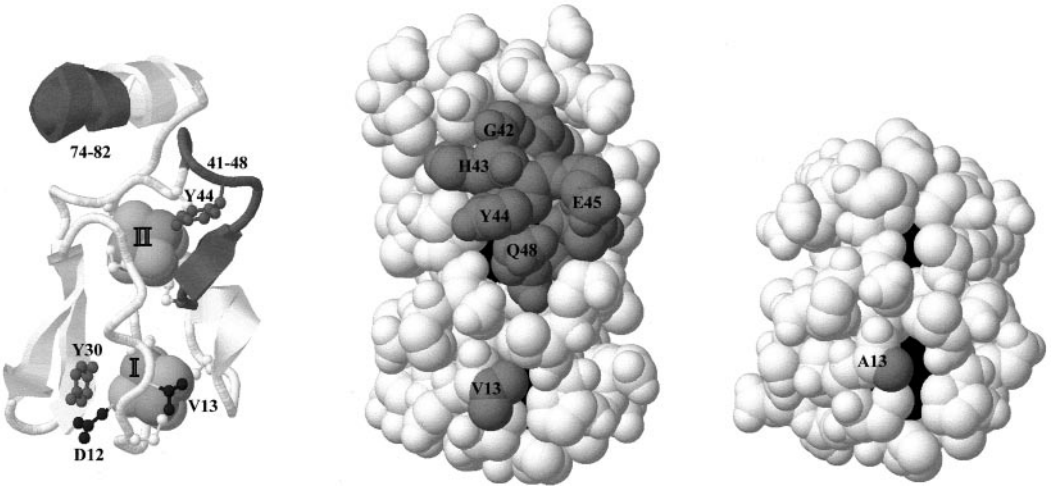

FIG. 1. **Structural comparison of 2[4Fe-4S] ferredoxins.** *Left*, cartoon of the structure of CvFd highlighting targets for site-directed mutagenesis. Cluster I coordinated by cysteines 8, 11, 14, and 53 lies at the bottom of the figure with nearby residues Val-13, Asp-12, and Tyr-30. Cluster II coordinated by cysteines 37, 40, 49, and 18 is close to the 41–48 loop with Tyr-44 (*upper right*) and the C-terminal part of the helix (residue 74–82, *top* of the figure). Space-filling representation of the structures of CvFd (Protein Data Base file 1BLU, *center*) and of *C. acidurici* Fd (Protein Data Base file 1FDN, *right*). The iron sulfur clusters are shown in *black*, and the loop 41–48 and the side chain in position 13 are shown in *dark gray*. The center view of CvFd is rotated 45° around a vertical axis relative to that on the *left*.

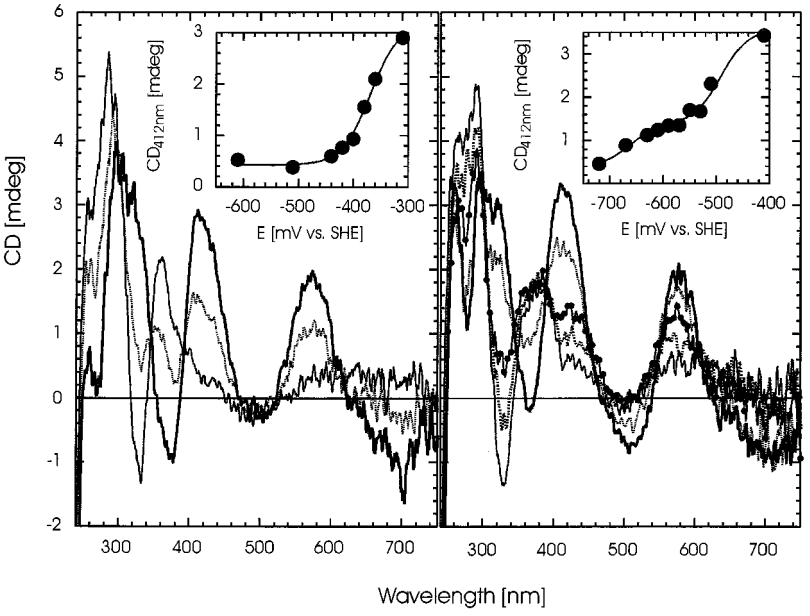

FIG. 2. **CD-monitored electrochemical redox titration of CpFd (*left*) and CvFd (*right*).** Spectra were recorded in an optically transparent thin layer electrode cell with a path length of 0.1 mm. Selected spectra at +90; −380 and −510 mV for CpFd and +100; −510; −610; −670 and −720 mV for CvFd (decreasing order of intensity at 412 nm, respectively) are shown. The *insets* contain Nernst curves calculated from the CD intensity at 412 nm and fitted with the following parameters: for CpFd, $n = 1$, $E^0 = -369$ mV; for CvFd, $n = 1$, $E^0_1 = -492$ mV, $E^0_2 = -663$ mV.

in the 300–800 nm range (Fig. 2). Therefore, the optical properties of the oxidized clusters of CvFd do not differ from typical $[4Fe\text{-}4S]^{2+}$ clusters, such as those of CpFd (Fig. 2). Below 300 nm, however, significant changes between CpFd and CvFd are noticed (Fig. 3). The relatively intense negative band around 220 nm in CvFd is indicative of the presence of the α-helix evidenced in the x-ray structure of the protein (10). This secondary structure element is absent in CpFd and has been found to produce different signatures when either the 2-turn loop or the α-helix are removed or modified in CvFd (not shown). Another difference between the two proteins occurs at 258 nm where a positive band is found in the spectra of CvFd but not in those of CpFd (Fig. 2).

The reductive titration of CvFd proceeds as for CpFd with a general decrease of the CD intensity when the potential is lowered (Fig. 2). Between approximately −550 mV and −600 mV, no further significant decreases are observed (Fig. 2); a midpoint potential of −492 ± 8 mV can be calculated which agrees with values determined by electrochemical measurements (Ref. 25 and see below) and redox titrations with dithionite (22, 23). However, the CD spectra obtained at potentials lower than this transition retain part of the features of the oxidized spectra, in contrast to what was observed with CpFd (Fig. 2). The CD spectra of CvFd did not show any decrease in intensity even after maintaining potentials in the −500 to −600 mV range for more than 1 h. Only a further decrease in potential succeeded in bleaching the CD spectra in the visible range, giving a spectroscopic signature very much like that of reduced CpFd (Fig. 2). A second midpoint redox potential at −663 ± 20 mV could be calculated from the latter part of the titration curve (Fig. 2, *inset*).

The spectral changes associated with the first and the second transitions differ significantly (Fig. 4). The prominent CD bands at 366 (negative) and 410 nm (positive) readily disappear during the first transition. The spectral features corresponding to the second transition at lower potential are less intense and compare with the intensity observed for ferredoxins having a single [4Fe-4S] cluster (11). A likely interpretation is that the interaction between the two [4Fe-4S] clusters, the closest metal atoms of which are less than 9 Å apart (2), contributes to the

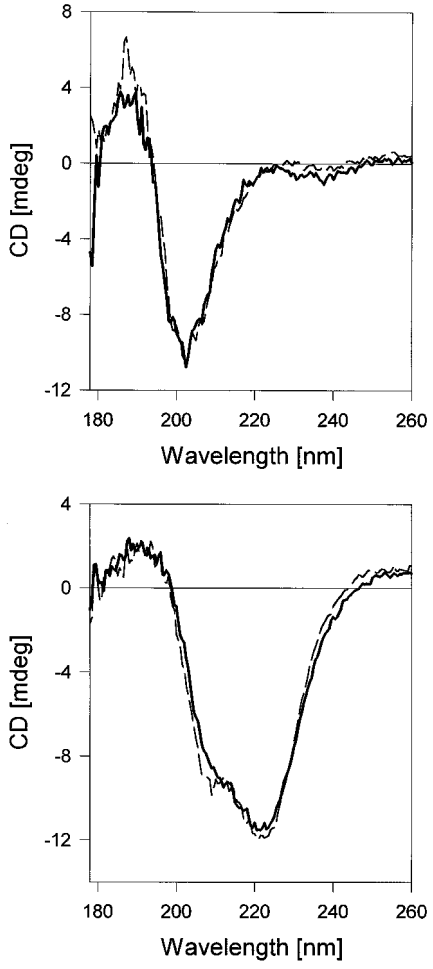

FIG. 3. **CD spectra of CpFd (*top*) and CvFd (*bottom*) in the UV range.** *Solid lines*, fully oxidized proteins (E = +0.1V for CpFd and −0.4 V for CvFd); *broken lines*, fully reduced proteins (E = −0.6 V for CpFd and −0.9 V for CvFd). The protein concentrations were 0.2 mM for CpFd and 0.15 mM for CvFd. The optical path length was 0.02 mm.

CD spectra of 2[4Fe-4S] ferredoxins; the pair of CD bands at 366 and 410 nm may therefore arise from exciton coupling between the strongest transitions observed in absorption spectra around 388 nm (Fig. 5) and assigned to S-Cys ⇒ Fe charge transfer bands (26). It should also be noted that the orientation (Fe-S-C-C and χ_1 dihedrals) of one cysteine ligand (Cys-40) is different for oxidized Cp and CvFd (10); this may change the CD features of cluster II, coordinated by Cys-40, and may explain the spectral differences between CpFd and CvFd, *i.e.* the intensity of the band at 258 nm in the oxidized state and the relative intensities of the bands at 360 and 380 nm in the reduced states.

As in the case of CpFd the CD spectra of CvFd in the UV region remain qualitatively the same at different reduction levels (Fig. 3). This observation provides evidence that in both ferredoxins the structural changes associated with the redox interconversion of the $[4Fe\text{-}4S]^{2+/+}$ clusters are minimal.

At the end of the reductive titrations, increasing the potential to 0 mV restored the initial spectrum recorded for each fully oxidized protein, hence indicating that the observed changes are fully reversible and that the implemented experimental conditions are not harmful to the integrity of these 2[4Fe-4S] ferredoxins.

Visible Absorption Spectroscopy

In order to sustain the above observations, the visible absorbance of CvFd was also monitored as a function of the

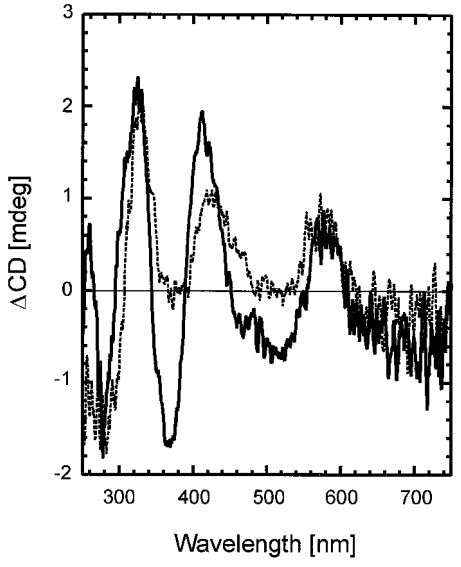

FIG. 4. **Difference CD spectra for the two redox transitions of CvFd.** *Solid line*, spectrum at −570 mV subtracted from that recorded at −100 mV; *broken line*, spectrum at −720 mV subtracted from that recorded at −570 mV.

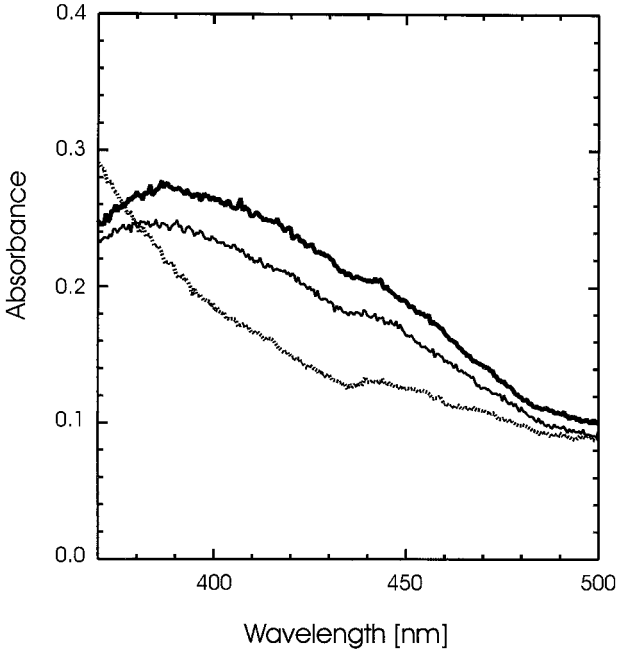

FIG. 5. **Absorption spectra of CvFd.** Spectra were recorded at −200 mV, *bold line*; −600 mV, *thin line*; −730 mV, *dotted line*. The protein concentration was 0.8 mM; the optical path length was 0.1 mm.

applied potential. The decrease of absorbance at 425 nm is a measure of the degree of reduction of $[4Fe\text{-}4S]^{2+/+}$ clusters, as the spectra of the reduced clusters are less intense than those of the oxidized ones (24). Fig. 5 shows the visible absorption spectra of oxidized (applied potential, E = −200 mV), partially (E = −600 mV), and fully reduced (E = −730 mV) CvFd. Dithionite appears as effective as electrochemical reduction at −600 mV (not shown) but does not provide the largest decrease in absorbance as judged by comparison with the spectrum recorded at −730 mV. Only the latter data agree with absorbance changes observed in a sample reduced by chloroplasts under illumination (8).

Thus, the above titrations carried out with CvFd strongly suggest that the protein displays two redox transitions. Qualitatively similar results were also obtained with molecular

TABLE II
Reduction potential of CvFd and molecular variants by CD titration and electrochemical studies

Ferredoxin	CD titration		Cyclic voltammetry		Square wave voltammetry	
	E_1	E_2	E_1	E_2	E_1	E_2
CpFd	−369 ± 4[a]		−392[b]		−405[b]	
CvFd	−492 ± 8[a]	−663 ± 20[a]	−461[b]	−653[b]	−453[b]	−658[b]
Δ1[c]			≈−417[d]	−640	—[e]	−663
K74−[c]			−431	−654	−439	−654
Δ1K74−[c]			−402	≈−651[d]	−424	—[e]
Y44C[f]	−478 ± 6	−627 ± 13[a]	−471	≈−653[d]	−468	—[e]
D12G	−482 ± 7[a]	−586 ± 11	−465[b]	−621[b]	−453[b]	−619[b]
V13G[f]			−478	−601	−475	−600
Y30F[b]			−463	−659	−458	−663

[a] Without salt.
[b] 0.15 M NaCl.
[c] 0.2 M NaCl.
[d] Broad anodic peak; the midpoint potential was estimated from the cathodic peak position.
[e] Two overlapping peaks observed in this potential region.
[f] 0.4 M NaCl.

variants of CvFd, and all reduction potential values are listed in Table II. However, such results may be biased, for instance by the involvement of a kinetic barrier slowing down the reduction of one cluster and apparently shifting the midpoint potential of the redox transition. This possibility has been addressed by additional experiments.

Reduction Potentials by Cyclic and Square Wave Voltammetries

Typical voltammograms of native CpFd and CvFd are shown in Fig. 6. CpFd shows only a single transition at approximately −400 mV, whereas CvFd shows two transitions at approximately −460 and −655 mV. The strong intensity of the single wave of CpFd agrees with the above observation that both [4Fe-4S] clusters react at this potential. Control experiments, with mediator mixtures (methyl viologen and 4′,4″-dimethyl-1′,1″trimethylene-2′,2″-dipyridinium dibromide) in the absence of protein, were carried out and showed that there is only a minor contribution of the mediator mixture to the electrochemical signal in the presence of the protein (Fig. 6). The reduction potentials determined for all forms studied are listed in Table II. From this series of measurements, it appears that the more negative value of CvFd redox potential (−655 mV) is shifted in variants with substitutions in the vicinity of cluster I, *i.e.* D12G and V13G; in these molecules the potential with the less negative value (−460 mV) agrees with the value measured for the native protein. Conversely, shifts of the less negative but not of the more negative redox potential were observed in variants, such as Δ1, K74−, and Δ1K74−, structurally modified around cluster II. These data indicate that the redox transition at −460 mV (native CvFd) arises from cluster II and the lowest transition at −655 mV is due to cluster I. Proteins carrying the C-terminal truncation displayed partially broadened and split electrochemical signals, so that some potentials could not be determined reliably. This electrochemical behavior correlates with a decreased stability of these proteins which was also observed during the CD-monitored redox titrations and other experiments (not shown). No significant changes were found for Y30F, as already observed with similar variants of other ferredoxins (27).

Kinetics of the Interaction between the Electrode and the Protein

2[4Fe-4S] ferredoxins show quasi-reversible electrode kinetics at the gold electrode in the presence of viologens up to scan rates of 1 V/s. At high scan rates, the separation between the anodic and the cathodic peak increased with increasing scan rate; from this, the heterogenous electron transfer rate constant k^0 (28) could be estimated (Table III), assuming a diffusion coefficient D = 10^{-6} cm^2/s which is consistent with the observed peak current. Quite remarkably, different electrode kinetics were observed for cluster I (E_m = −655 mV) and cluster II (E_m = −460 mV); the heterogenous rate constant for the oxido-reduction of the latter was determined as approximately 4 × 10^{-3} cm/s, whereas the former showed reversible electrode kinetics up to scan rates of 0.5 V/s. Therefore, a lower limit of 2 × 10^{-2} cm/s was estimated for the heterogenous rate constant of cluster I in all variants studied. These values support the statement that no fast electron transfer takes place between the clusters (7); otherwise, oxidoreduction of both clusters could proceed rapidly via cluster I.

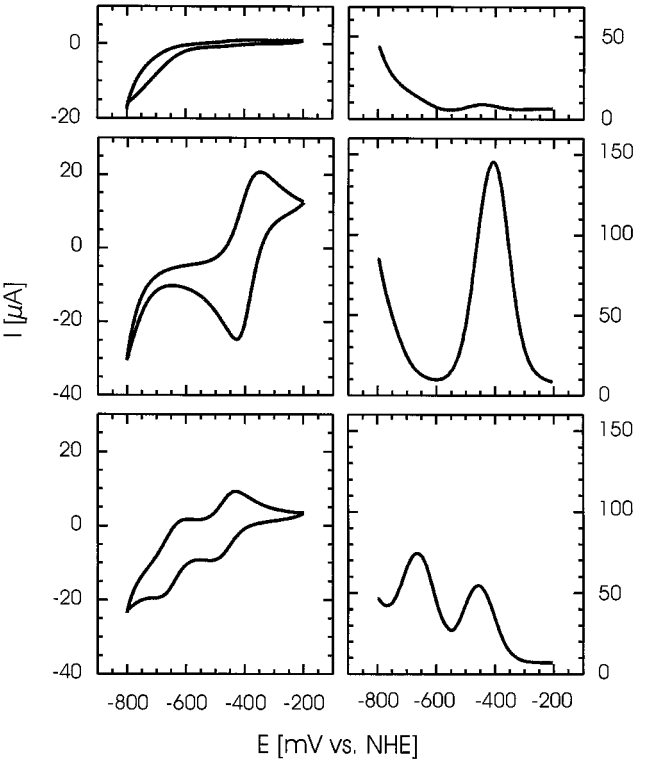

FIG. 6. **Electrochemical characterization of CpFd and CvFd.** Cyclic (*left*) and square wave (*right*) voltammograms of the buffer control with viologen mediators added (*top*), CpFd (*middle*), and CvFd (*bottom*). Cyclic voltammograms were taken at 25 °C and at a potential scan rate of 10 mV/s. Square wave voltammograms were taken at 25 °C and a frequency of 8 Hz with a step potential of 5 mV and an amplitude of 50 mV.

Electron transfer to cluster II is faster in the Δ1 and Δ1K74− forms in which it is comparable to electron transfer to cluster I. This result is consistent with dithionite reduction kinetics dis-

TABLE III
Kinetics of reduction of native CvFd and molecular variants

Ferredoxin	Heterogenous electron transfer rate, k^0 of cluster II	Homogeneous rate constant for the reduction (of cluster II) by dithionite
	cm/s	$M^{-1/2}\ s^{-1}$
Native CvFd	$4 \cdot 10^{-3}$	0.02
Y30F	$(4–8) \cdot 10^{-3}$	0.02
Y44S		0.03
Y44C	$11 \cdot 10^{-3}$	
D12G	$8 \cdot 10^{-3}$	0.03
K74E		$\gg$0.2
K74−	$3 \cdot 10^{-3}$	$\gg$0.2
Δ1	$>2 \cdot 10^{-2}$	$\gg$0.2
Δ1K74−	$>10^{-2}$	$\gg$0.2
CpFd	$6 \cdot 10^{-3}$	19[a]

[a] Value from data obtained by stopped-flow measurements (52).

cussed below. The other structural changes studied in this work had less significant effects on the electron transfer kinetics except for Y44C which displayed an increased heterogenous rate constant by a factor of approximately 3-fold. It is conceivable that cysteine in this position facilitates electron transfer to and from cluster II by interacting with the gold electrode or that the removal of the aromatic ring makes cluster II more exposed.

Surprisingly, the heterogenous rate constant determined for CpFd, which agrees with previously reported ones (29, 30), is closer to those of CvFd cluster II than to those of CvFd cluster I (Table III). This is another noteworthy difference between the latter and CpFd clusters, despite their structural similarity (10).

Effect of Ionic Strength and pH

The effect of ionic strength on the values of the reduction potential of native CvFd has been measured in solutions with NaCl concentrations up to 1 M. A linear relationship between the redox potential and the square root of the ionic strength was observed over the whole range studied with a slope of +35 mV/$M^{0.5}$ for both clusters. The variation is similar to that obtained in previous studies on $[4Fe\text{-}4S]^{2+/+}$ clusters in other proteins (23).

The effect of pH has also been studied. At pH values equal to or below 6, the electrochemical response was not satisfactory in the implemented conditions. Although the ionic strength was not kept constant at the different pH values, the weak dependence with ionic strength observed at pH 7.5 dismisses a major contribution of this parameter. Only at pH values above 10 do the reduction potentials of both transitions significantly shift; these data may indicate the binding of hydroxide ions to the clusters and associated changes in their electronic properties. At these high pH values, structural modifications of the protein must also be considered. The case of cluster II is interesting because, in contrast to cluster I, this group displays an increase of the redox potential with increasing pH opposite to the effect of electrostatic repulsion between the $[Fe_4S_4(Cys)_4]^{2-/3-}$ cluster and nearby deprotonated residues, such as His-43.

Kinetics of Dithionite Reduction of CvFd

From the comparison of the absorption spectra described above, dithionite appears to be able to reduce only cluster II in CvFd. The decrease with time of the absorbance at 425 nm has been analyzed as a pseudo first-order kinetic process; the rate constants calculated using the added dithionite concentration are listed in Table III. It is easily concluded that in the molecular variants missing either loop Δ1 or half of the C terminus α-helix, reduction of cluster II takes place at least 10 times faster compared with native CvFd.

The same kinetic effect is also observed in the case of K74E, thus providing evidence of significant structural changes around cluster II in molecules in which Lys-74 is changed. The side chain of Lys-74 is involved in stabilizing interactions around cluster II (10), and its replacement or its removal are expected to perturb the structural environment of cluster II. Despite the similarities observed between the kinetics of dithionite and electrode reduction of the molecules listed in Table III, these reactions do not exactly obey the same mechanism as shown by the qualitative differences exhibited by CpFd and cluster II of CvFd Lys-74 variants (slow electrode kinetics and fast dithionite reduction).

DISCUSSION

The results presented herein reveal a difference of approximately 200 mV between the reduction potentials of the clusters in a 2[4Fe-4S] ferredoxin. Although previous studies were conducted with CvFd (22, 23), including studies under experimental conditions very similar to those implemented here (25), the very negative redox transition exhibited by CvFd escaped detection.

Existence of Two Redox Transitions—The voltammograms of CvFd and all studied derivatives consistently showed the occurrence of two redox transitions in these proteins. The CD redox titrations fully agree with these conclusions: very similar CD spectra were obtained for reduced CpFd and CvFd, but although the oxidized spectra of the former protein readily disappeared at −500 mV, those of the latter required potentials below −700 mV. Similarly, the decrease in absorbance at 425 nm exhibited by CpFd upon dithionite reduction (~55%, see Refs. 23 and 31) could only be reached by applying a potential of −730 mV in the case of CvFd. Dithionite reduction of the latter protein resulted in a decrease of ~25%, *i.e.* a value roughly half of that corresponding to full reduction. Therefore, two independent methods of investigation, voltammetry and optical titrations, point toward the involvement of two distinct redox transitions in the case of CvFd. Furthermore, the spectroscopic features observed in the course of the potentiometric titrations showed no evidence for cluster interconversion, from a [4Fe-4S] to a [3Fe-4S] cluster for instance, a now largely documented occurrence in [4Fe-4S] proteins (32). Indeed, the close similarity of the CD spectra recorded with CpFd and CvFd and the reversibility of the CD-monitored titration do indicate that the clusters remain in the [4Fe-4S] form during these experiments and that the electrochemical signals have to be attributed to the redox properties of genuine [4Fe-4S] clusters. The formation of $[3Fe\text{-}4S]^{+/0}$ clusters is expected to be accompanied by the development of an intense CD band around 450 nm as in the case of mitochondrial aconitase (33), which has never been detected in our experiments. The electrochemical observation of separate redox waves has very recently been obtained with a newly isolated 2[4Fe-4S] ferredoxin from *Azotobacter vinelandii* apparently bearing strong structural similarities with the proteins investigated herein, but the two redox transitions have not been assigned, and no structural reasons for their occurrence have been put forward (34).

A direct implication of the presence of two redox transitions in CvFd is that the previously reported spectroscopic data using magnetic resonances (7) have to be reinterpreted considering that only one cluster (cluster II) was efficiently reduced by dithionite. Such studies are under way and will reveal how the magnetic properties of a diamagnetic $[4Fe\text{-}4S]^{2+}$ cluster (cluster I) are perturbed by the presence of a paramagnetic $[4Fe\text{-}4S]^{+}$ cluster (cluster II) nearby.

Assignment of the Redox Transitions to the Two Clusters—The two redox transitions of CvFd are sensitive to some extent to the modifications introduced in the sequence of the protein (Table II). Remarkably enough, the lowest potential transition is affected when amino acids close to cluster I are changed, whereas the less negative one more specifically responds to

TABLE IV
Reduction potential values of [4Fe-4S] clusters bound to different $CX^1X^2CX^3X^4C$ motifs in 2[4Fe-4S] and [4Fe-4S][3Fe-4S] ferredoxins

Species/ferredoxin	X^3	X^4	E ([4Fe-4S])	Refs.[a]
Escherichia coli	Asp	Met	−680	This work
Chromatium vinosum	Asp	Val	−655	This work
A. vinelandii/FdIII	Asp	Val	−644	34
Pseudomonas nautica ($)[b]	Ala	Leu	−680	53
A. vinelandii/FdI ($)	Ala	Leu	−647	39
R. capsulatus/FdII ($)	Gly	Val	−640	54
Sulfolobus sp. strain 7 ($)	Met	Ala	−530	55
Rhodobacter capsulatus/FdI	Gly	Asp	−490	45
Desulfovibrio africanus/FdIII ($)	Glu	Ser	−430	56
Clostridial cluster I	Gly	Ala or Ser	Around −400	4, 23, 25, 27, 31
Clostridial cluster II	Gly	Asn or Ser or Ala	Around −400	
Entamoeba histolytica	Gly	Ala	−320	27
Methanosarcina barkeri	Gly	Thr	−320	57

[a] All sequences were retrieved from the sequence data bases.
[b] The $ indicates [3Fe-4S][4Fe-4S] ferredoxins.

replacements introduced close to cluster II. These assignments are supported by additional spectroscopic evidence to be reported elsewhere. This brings forth the surprising conclusion that the cluster of CvFd (cluster II), the environment of which was shown by comparison of oxidized x-ray structures to differ most from that of clusters in clostridial ferredoxins, exhibits a moderate shift in potential of approximately −60 mV, whereas the other cluster for which no obvious structural difference was detected at this level of resolution displays a huge negative shift of about −250 mV.

The factors determining the values of redox potentials in metallo- and other redox active proteins still remain somewhat obscure in many cases. The most sophisticated theoretical approaches currently available attempt at considering all electrostatic contributors to the energy of the solvated protein, at both redox levels, on the microscopic scale (35). In the cases of a few metalloprotein classes, one particular parameter accounts for a good deal of the observed shifts among natural or artificially produced variants of the class; for example, solvation of the $[4Fe\text{-}4S]^{3+/2+}$ clusters was proposed as a major contributor to the modulation of the redox potential in high potential ferredoxins (36). In contrast, a delicate balance of interactions seems relevant in other cases (37). One such example was provided by $[4Fe\text{-}4S]^{2+/+}$ clusters in proteins for which no convincing evidence for the involvement of one major parameter was available (*e.g.* Refs. 4 and 38). Redox potential shifts have been occasionally observed upon extensive rearrangement around $[4Fe\text{-}4S]^{2+/+}$ clusters (39). The present results give the opportunity to address this question further by including the experimental data on CvFd.

Factors Contributing to the Reduction Potential of Cluster II—From the comparison of the values measured with native CpFd, and with the Δ1, K74−, and Δ1K74− variants (Table II), the loop between Cys-40 and Cys-49 and the C terminus α-helix clearly contribute to the negative shift of the potential of cluster II compared with CpFd. When the two structural features are removed in Δ1K74−, the reduction potential difference is almost completely abolished, showing that a structural environment very similar to that in CpFd has thus been engineered around cluster II in CvFd. It is likely that a hydrogen bond equivalent to that between Gly-41 NH (or Gly-12 NH) and one inorganic sulfur in clostridial type ferredoxins (21) that is absent in native CvFd (10) has been recovered in Δ1K74−.

The significant kinetic effect of the dithionite reduction of cluster II in the variants Δ1, K74−, and Δ1K74− (Table III) may be correlated with the degree of accessibility of cluster II, one of the parameters that is often put forward to explain reduction potential values in proteins containing [4Fe-4S] clusters. Although no crystal structure of the variants are yet available, Fig. 1 shows that the loop 41–48 contributes to shield cluster II from the solvent and may impair the reactivity of even small anions, like dithionite, with this cluster.

Why Is the Potential of Cluster I So Negative?—The very low potential redox transition in CvFd has been assigned to cluster I based on the absence of significant potential shifts in the case of molecules bearing changes close to cluster II and on a selective shift in the case of the D12G and V13G (Table II) modifications around cluster I. The only marginal (approximately 15 mV) exceptions are for molecules missing the Δ1 loop which may undergo a general adjustment of the protein structure. Contrary to the case of cluster II, no obvious structural features distinguish CvFd cluster I from the clusters of clostridial ferredoxins (10). The exposed side chain of Asp-12 contributes some 30 mV to the value of the potential of cluster I in CvFd, in a way reminiscent, but probably not identical (see below), to the case of the H35D/D41H form of *A. vinelandii* ferredoxin I (38).

Values of reduction potentials for [4Fe-4S] clusters similar to that of cluster I in CvFd have yet been determined only in the case of one 2[4Fe-4S] and in some [3Fe-4S][4Fe-4S] ferredoxins (Table IV). They have also been suspected for [4Fe-4S] clusters, the role of which may be to serve as oxygen sensors, like in *Bacillus subtilis* glutamine phosphoribosylpyrophosphate amidotransferase (40) or *E. coli* fumerate and nitrate reductase regulation transcription factor (41). Even lower values were predicted for the non-physiological 2+/+ transition of [4Fe-4S] clusters in high potential ferredoxins and in *E. coli* endonuclease III (42). The structures of oxidized *Peptostreptococcus asaccharolyticus* ferredoxin and of *A. vinelandii* ferredoxin I have been used to calculate the reduction potential of the [4Fe-4S] clusters in these proteins (43). The 250 mV less negative potential in the former was explained by the occurrence of additional Langevin dipoles in the vicinity of cluster I in *P. asaccharolyticus* ferredoxin. It should be noted, however, that the atomic resolution (0.94 Å) structure of *Clostridium acidurici* Fd, a protein very similar in structure and reduction potential values to *P. asaccharolyticus* ferredoxin, did not exhibit these Langevin dipoles as crystallized water molecules (2). Therefore, the experimental evidence sustaining the theoretical conclusions is still missing, but, because CvFd provides significant new information, a thorough comparison of the sequence and electrochemical data available for [4Fe-4S] clusters of homologous 2[4Fe-4S] and [4Fe-4S][3Fe-4S] ferredoxins in the literature has been conducted (Table IV). A correlation appears between the presence of a bulky non-polar side chain in position X^4 (Leu, Val, and Met) of the $CX^1X^2CX^3X^4C$ coordinating triad and the very negative potential of the associated [4Fe-4S] cluster. Fig. 1 shows that cluster I should become more exposed if the side chain of valine 13 is replaced by a smaller residue, like the alanine found in *C. acidurici* ferredoxin. This effect has been probed in CvFd by V13G substitution. As expected from

the data of Table IV, the potential of cluster I is significantly less negative than that of the native protein (Table II). Therefore, the amino acid in position X^4 of the coordinating sequence modulates the potential of [4Fe-4S] clusters. However, the observed shift does not fully explain the approximate 250 mV decrease in potential of CvFd cluster I compared with the clusters of CpFd. Clearly, additional contributors will have to be discovered before understanding the molecular details setting the redox potential values in [4Fe-4S] proteins.

Comparisons with Other Proteins—To date only a few 2[4Fe-4S] domains in proteins have been reported to contain clusters with different values of reduction potentials. These range from moderate differences as in subunit PsaC of photosystem I (44) and a molecular variant of *Rhodobacter capsulatus* 2[4Fe-4S] ferredoxin (45), up to larger ones in the cases of *E. coli* nitrate reductases A and Z (46) and dimethyl sulfoxide reductase (47). Since CvFd is well characterized (7, 9, 10), it could now become a standard model to study the above unusual redox properties, all the more so as proteins of this family display the largest potential difference among all these examples. The quest for a rationale to the very negative value of the potential of CvFd cluster I may also benefit from previous observations made with other systems containing low potential (<-600 mV) [4Fe-4S]$^{2+/+}$ clusters, such as center Fx of photosystem I (44) or the nitrogenase Fe protein (48).

Functional Consequences—The function or the redox partners of CvFd are not known, and only some hypotheses have been put forward in the past (49). Contrary to other 2[4Fe-4S] ferredoxins, CvFd is unable to couple electron transfer between *C. pasteurianum* pyruvate-ferredoxin oxidoreductase and hydrogenase, although the reduction potential of its cluster II lies in the range considered suitable to fulfill this function (50). In the light of the findings presented here (very low potential of cluster I), CvFd behaves in this assay like ferredoxins containing a single [4Fe-4S] cluster. This may indicate that the two nearly isopotential and symmetrical clusters of 2[4Fe-4S] ferredoxins are necessary to complete an efficient electron transfer chain between these enzymes.

The demonstration of an extremely low potential [4Fe-4S] cluster belonging to a tandem of such closely spaced centers has further consequences. For instance, the exact stoichiometry of Fe-S centers in a number of NADH-ubiquinone oxidoreductases remains a matter of some dispute (51), mainly because of the discrepancies between the potential coordinating motifs found in sequences and the relatively low number of signals detected with various spectroscopies. It seems possible that if some of the clusters present in these complex systems display properties similar to those of cluster I of CvFd, they may easily escape observation, hence accounting for part of the discrepancies. It will then be important to establish the functional role of such clusters, and the study of relatively simple molecules like the ferredoxins investigated in the present work may prove easier to fulfill this goal than that of complicated enzymes, such as complex I of the mitochondrial respiratory chain.

Acknowledgments—Professor B. K. Burgess is thanked for communicating unpublished data. Discussions with Professor R. Cammack about the early characterization of CvFd and the content of the manuscript have been very useful. Dr J. Meyer is thanked for reading the manuscript.

REFERENCES

1. Matsubara, H., and Saeki, K. (1992) *Adv. Inorg. Chem.* **38,** 223–280
2. Dauter, Z., Wilson, K. S., Sieker, L. C., Meyer, J., and Moulis, J.-M. (1997) *Biochemistry* **36,** 16065–16073
3. Otaka, E., and Ooi, T. (1987) *J. Mol. Evol.* **26,** 257–267
4. Quinkal, I., Davasse, V., Gaillard, J., and Moulis, J.-M. (1994) *Protein Eng.* **7,** 681–687
5. Stout, G. H., Turley, S., Sieker, L. C., and Jensen, L. H. (1988) *Proc. Natl. Acad. Sci. U. S. A.* **85,** 1020–1022
6. Beinert, H., and Thomson, A. J. (1983) *Arch. Biochem. Biophys.* **222,** 333–361
7. Huber, J. G., Gaillard, J., and Moulis, J.-M. (1995) *Biochemistry* **34,** 194–205
8. Bachofen, R., and Arnon, D. I. (1966) *Biochim. Biophys. Acta* **120,** 259–265
9. Moulis, J.-M. (1996) *Biochim. Biophys. Acta* **1308,** 12–14
10. Moulis, J.-M., Sieker, L. C., Wilson, K. S., and Dauter, Z. (1996) *Protein Sci.* **5,** 1765–1775
11. Stephens, P. J., Thomson, A. J., Dunn, J. B. R., Keiderling, T. A., Rawlings, J., Rao, K. K., and Hall, D. O. (1978) *Biochemistry* **17,** 4770–4778
12. Link, T. A., Hatzfeld, O. M., Unalkat, P., Shergill, J. K., Cammack, R., and Mason, J. R. (1996) *Biochemistry* **35,** 7546–7552
13. Meyer, J., Fujinaga, J., Gaillard, J., and Lutz, M. (1994) *Biochemistry* **33,** 13642–13650
14. Sanger, F., Nicklen, S., and Coulson, A. R. (1977) *Proc. Natl. Acad. Sci. U. S. A.* **74,** 5463–5467
15. Tabor, S. (1990) in *Current Protocols in Molecular Biology* (Ausubel, F. A., Brent, R., Kingston, R. E., Moore, D. D., Seidman, J. G., Smith, J. A., and Struhl, K., eds) pp. 16.2.1–16.2.11, Greene Publishing and Wiley Interscience, New York
16. Moulis, J.-M., Davasse, V., and DeJésus, F. (1994) *Biometals* **7,** 272–278
17. Davasse, V., and Moulis, J.-M. (1992) *Biochem. Biophys. Res. Commun.* **185,** 341–349
18. Hagen, W. R. (1989) *Eur. J. Biochem.* **182,** 523–530
19. Salmon, R. T., and Hawkridge, F. M. (1980) *J. Electroanal. Chem.* **112,** 253–264
20. George, S. J., Thomson, A. J., Crabtree, D. E., Meyer, J., and Moulis, J.-M. (1991) *New J. Chem.* **15,** 455–465
21. Duée, E. D., Fanchon, E., Vicat, J., Sieker, L. C., Meyer, J., and Moulis, J.-M. (1994) *J. Mol. Biol.* **243**, 683–695
22. Ke, B., Bulen, W. A., Shaw, E. R., and Breeze, R. H. (1974) *Arch. Biochem. Biophys.* **162,** 301–309
23. Stombaugh, N. A., Sundquist, J. E., Burris, R. H., and Orme-Johnson, W. H. (1976) *Biochemistry* **15,** 2633–2641
24. Sweeney, W. V., and Rabinowitz, J. C. (1980) *Annu. Rev. Biochem.* **49,** 139–161
25. Smith, E. T., and Feinberg, B. A. (1990) *J. Biol. Chem.* **265,** 14371–14376
26. Moulis, J.-M., Meyer, J., and Lutz, M. (1984) *Biochemistry* **23,** 6605–6613
27. Quinkal, I., Kyritsis, P., Kohzuma, T., Im, S.-C., Sykes, A. G., and Moulis, J.-M. (1996) *Biochim. Biophys. Acta* **1295,** 201–208
28. Nicholson, R. S. (1965) *Anal. Chem.* **37,** 1351–1355
29. Van Dijk, C., van Eijs, T., van Leeuwen, J. W., and Veeger, C. (1984) *FEBS Lett.* **166,** 76–80
30. Armstrong, F. A., Cox, P. A., Hill, H. A. O., Lowe, V. J., and Oliver, B. N. (1987) *J. Electroanal. Chem.* **217**, 331–366
31. Moulis, J.-M., and Meyer, J. (1982) *Biochemistry* **21,** 4762–4771
32. Beinert, H. (1990) *FASEB J.* **4,** 2483–2491
33. Piszkiewicz, D., Gawron, O., and Sutherland, J. C. (1981) *Biochemistry* **20,** 363–366
34. Gao-Sheridan, H. S., Pershad, H. R., Armstrong, F. A., and Burgess, B. K. (1998) *J. Biol. Chem.* **273,** 5514–5519
35. Warshel, A., Papazyan, A., and Muegge, I. (1997) *J. Biol. Inorg. Chem.* **2,** 143–152
36. Heering, H. A., Bulsink, Y. B. M., Hagen, W. R., and Meyer, T. E. (1995) *Biochemistry* **34,** 14675–14686
37. Mauk, A. G., and Moore, G. R. (1997) *J. Biol. Inorg. Chem.* **2,** 119–125
38. Shen, B., Jollie, D. R., Stout, C. D., Diller, T. C., Armstrong, F. A., Gorst, C. M., La Mar, G. N., Stephens, P. J., and Burgess, B. K. (1994) *J. Biol. Chem.* **269,** 8564–8575
39. Iismaa, S. E., Vázquez, A. E., Jensen, G. M., Stephens, P. J., Butt, J. N., Armstrong, F. A., and Burgess, B. K. (1991) *J. Biol. Chem.* **266,** 21563–21571
40. Vollmer, S. J., Switzer, R. L., and Debrunner, P. G. (1983) *J. Biol. Chem.* **258,** 14284–14293
41. Khoroshilova, N., Popescu, C., Münck, E., Beinert, H., and Kiley, P. J. (1997) *Proc. Natl. Acad. Sci. U. S. A.* **94,** 6087–6092
42. Stephens, P. J., Jollie, D. R., and Warshel, A. (1996) *Chem. Rev.* **96,** 2491–2513
43. Jensen, G. M., Warshel, A., and Stephens, P. J. (1994) *Biochemistry* **33,** 10911–10924
44. Brettel, K. (1997) *Biochim. Biophys. Acta* **1318,** 322–373
45. Saeki, K., Tokuda, K., Fukuyama, K., Matsubara, H., Nadanami, K., Go, M., and Itoh, S. (1996) *J. Biol. Chem.* **271,** 31399–31406
46. Guigliarelli, B., Asso, M., More, C., Augier, V., Blasco, F., Pommier, J., Giordano, G., and Bertrand, P. (1993) *Eur. J. Biochem.* **207,** 61–68
47. Cammack, R., and Weiner, J. H. (1990) *Biochemistry* **29,** 8410–8416
48. Lanzilotta, W. N., and Seefeldt, L. C. (1997) *Biochemistry* **36,** 12976–12983
49. Evans, M. C. W., Buchanan, B. B., and Arnon, D. I. (1966) *Proc. Natl. Acad. Sci. U. S. A.* **55,** 928–934
50. Moulis, J.-M., and Davasse, V. (1995) *Biochemistry* **34,** 16781–16788
51. Albracht, P. J. S., and De Jong, A. M. P. (1997) *Biochim. Biophys. Acta* **1318,** 92–106
52. Lambeth, D. O., and Palmer, G. (1973) *J. Biol. Chem.* **248,** 6095–6103
53. Macedo, A. L., Besson, S., Moreno, C., Fauque, G., Moura, J. J. G., and Moura, I. (1996) *Biochem. Biophys. Res. Commun.* **229,** 524–530
54. Armengaud, J. (1994) *Caractérisetion structurale et functionelle des ferrédoxines II et IV de Rhodobacter capsulatus.* Ph.D thesis, Université Joseph-Fourier, Grenoble, France
55. Iwasaki, T., Wakagi, T., Isogai, Y., Tanaka, K., Iizuta, T., and Oshima, T. (1994) *J. Biol. Chem.* **269,** 29444–29450
56. Armstrong, F. A., George, S. J., Cammack, R., Hatchikian, E. C., and Thomson, A. J. (1989) *Biochem. J.* **264,** 265–273
57. Daas, P. J. H., Hagen, W. R., Keltjens, J. T., and Vogels, G. D. (1994) *FEBS Lett.* **356,** 342–344